DOI: 10.1534/genetics.105.049478

Mutations in Mre11 Phosphoesterase Motif I That Impair *Saccharomyces cerevisiae* Mre11-Rad50-Xrs2 Complex Stability in Addition to Nuclease Activity

Berit O. Krogh,[1] Bertrand Llorente,[1,2] Alicia Lam and Lorraine S. Symington[3]

Institute of Cancer Research and Department of Microbiology, Columbia University Medical Center, New York, New York 10032

Manuscript received May 17, 2005
Accepted for publication August 29, 2005

ABSTRACT

The Mre11-Rad50-Xrs2 complex is involved in DNA double-strand break repair, telomere maintenance, and the intra-S phase checkpoint. The Mre11 subunit has nuclease activity *in vitro*, but the role of the nuclease in DNA repair and telomere maintenance remains controversial. We generated six *mre11* alleles with substitutions of conserved residues within the Mre11-phosphoesterase motifs and compared the phenotypes conferred, as well as exonuclease activity and complex formation, by the mutant proteins. Substitutions of Asp16 conferred the most severe DNA repair and telomere length defects. Interactions between Mre11-D16A or Mre11-D16N and Rad50 or Xrs2 were severely compromised, whereas the *mre11* alleles with greater DNA repair proficiency also exhibited stable complex formation. At all of the targeted residues, alanine substitution resulted in a more severe defect in DNA repair compared to the more conservative asparagine substitutions, but all of the mutant proteins exhibited <2% of the exonuclease activity observed for wild-type Mre11. Our results show that the structural integrity of the Mre11-Rad50-Xrs2 complex is more important than the catalytic activity of the Mre11 nuclease for the overall functions of the complex in vegetative cells.

THE *RAD50, XRS2,* and *MRE11* genes were first identified in screens for ionizing radiation (IR)-sensitive or meiotic recombination-defective mutants in *Saccharomyces cerevisiae* (Symington 2002). Subsequent studies revealed similar defects in meiosis, repair of IR-induced DNA damage, telomere length, nonhomologous end joining (NHEJ), and the intra-S phase checkpoint in *mre11*, *rad50*, and *xrs2* null mutants (Haber 1998; D'Amours and Jackson 2002). The corresponding proteins form a high-affinity complex with an ~2:2:1 stoichiometry of Mre11, Rad50, and Xrs2 (Anderson *et al.* 2001; Chen *et al.* 2001). Both Mre11 and Rad50 are conserved and are homologous to the *Escherichia coli* SbcD and SbcC proteins, respectively (Sharples and Leach 1995). Functional analogs of the Xrs2 subunit are found only in eukaryotes, *e.g.*, the human Nbs1 protein, and the sequences of these display very limited interspecies homology (Carney *et al.* 1998; Varon *et al.* 1998; Chahwan *et al.* 2003; Ueno *et al.* 2003). Mre11 contains five sequence motifs found in a superfamily of phosphoesterases that, apart from *E. coli* SbcD, also includes di-metal Ser/Thr protein phosphatases. Conserved residues within these motifs are required for Mre11 nuclease activity *in vitro* (Furuse *et al.* 1998; Usui *et al.* 1998; Moreau *et al.* 1999). Mre11 displays 3′–5′ ssDNA, 3′–5′ dsDNA exonuclease, and ssDNA endonuclease activities with the endonuclease activity acting preferentially at ssDNA/dsDNA transitions (Furuse *et al.* 1998; Paull and Gellert 1998; Usui *et al.* 1998; Moreau *et al.* 1999; Trujillo and Sung 2001). Biochemical analyses of the Mre11-Rad50 complex suggest that one function of the complex is to tether DNA ends together (Chen *et al.* 2001; de Jager *et al.* 2001; Hopfner *et al.* 2002), and it has been suggested that this tethering activity could hold sister chromatids in close proximity for efficient repair (Wiltzius *et al.* 2005). The rapid recruitment of the Mre11-Rad50-Xrs2 (MRX) complex to double-strand breaks (DSBs) *in vivo* is critical for signaling DNA damage to downstream effectors, such as Tel1 and Mec1 in yeast or ATM in mammalian cells (Nelms *et al.* 1998; Grenon *et al.* 2001; Usui *et al.* 2001; Nakada *et al.* 2003; Uziel *et al.* 2003; Costanzo *et al.* 2004; Lisby *et al.* 2004).

The rapid recruitment of the Mre11 complex to DSBs is also suggestive of an early role in the repair of DSBs. Studies with the *mre11* null (*mre11*Δ) mutant have shown a defect in the 5′–3′ resection of DSBs suggesting a direct role of Mre11 in the nucleolytic resection process (Lee *et al.* 1998; Tsubouchi and Ogawa 1998). Although the exonuclease activity of Mre11 is of the opposite polarity to that observed for DSB resection (White and Haber 1990), the endonuclease activity of Mre11 could

[1]These authors contributed equally to this work.

[2]*Present address:* Institut Pasteur, Département des Biotechnologies, 28 rue du Dr. Roux, 75015 Paris, France.

[3]*Corresponding author:* Institute of Cancer Research and Department of Microbiology, Columbia University Medical Center, 701 W. 168th St., New York, NY 10032. E-mail: lss5@columbia.edu

potentially function in concert with a helicase unwinding the DNA duplex and the Mre11 endonuclease resecting the 5′ ends.

Analysis of *mre11* nuclease-defective (*mre11-nd*) mutants has led to conflicting views on the role of the Mre11 nuclease in end resection because of the different phenotypes conferred by these alleles. All of the *mre11-nd* mutants share the property of sporulation deficiency due to an inability to process Spo11-induced DSBs during meiosis, as well as synthetic mitotic lethality with *rad27*Δ (Furuse *et al.* 1998; Tsubouchi and Ogawa 1998; Usui *et al.* 1998; Moreau *et al.* 1999; Debrauwere *et al.* 2001). The Mre11-58 protein has two point mutations in phosphoesterase motif IV (H213Y, L225I), consistently lacks nuclease activity *in vitro*, and is furthermore defective in complex formation with Rad50 and Xrs2 (Usui *et al.* 1998). The *mre11-58* allele confers a phenotype similar to that of an *mre11*Δ allele for sensitivity to ionizing radiation, processing of HO-induced DSBs, and sensitivity to HU and telomere length, but is proficient for meiotic DSB formation (Tsubouchi and Ogawa 1998; Usui *et al.* 1998; D'Amours and Jackson 2001). The *mre11-D16A* mutant (phosphoesterase motif I) is less sensitive to IR than the *mre11*Δ mutant and the telomeres are of intermediate length between the *mre11*Δ and *MRE11* strains (Furuse *et al.* 1998). This mutant is proficient for end-joining repair of cohesive ends, and the purified Mre11-D16A protein interacts with Rad50 and Xrs2 *in vitro* (Lewis *et al.* 2004). However, the recruitment of Rad50 to telomeres is impaired in the *mre11-D16A* strain and there is a defect in complex formation between the *Schizosaccharomyces pombe* Rad32-D25A protein (equivalent to Mre11-D16A) and Rad50 *in vivo* (Tomita *et al.* 2003; Takata *et al.* 2005). In contrast, the *mre11-D56N* and *mre11-H125N* strains (phosphoesterase motifs II and III, respectively) show only a three- to fourfold decrease in survival to 500 Gy IR compared to *MRE11* strains, exhibit no defect in processing HO-induced DSBs, and have telomeres of the same length as *MRE11* strains (Moreau *et al.* 1999; Llorente and Symington 2004). These results have led to the suggestion that the Mre11-D56N and Mre11-H125N proteins retain sufficient residual nuclease activity to process DSBs *in vivo* (Lewis *et al.* 2004). However, in genetic assays for endonucleolytic processing of hairpin structures in yeast, the *mre11-D56N* and *mre11-H125N* strains were as defective as the *mre11*Δ strain, indicating that there is little, if any, residual endonuclease activity (Rattray *et al.* 2001; Lobachev *et al.* 2002; Farah *et al.* 2005). Biochemical studies of the human Mre11-3 protein, which has two amino acid substitutions within phosphoesterase motif III, have shown a complete loss of nuclease activity even though in the crystal structure of the *Pyrococcus furiosus* Mre11-3, the overall protein fold and active site conformation is the same as those in the wild-type protein (Arthur *et al.* 2004). *In vivo*, the yeast *mre11-3* mutant shows similar sensitivity to IR as the *mre11-H125N* strain and normal resection of an HO-induced DSB (Bressan *et al.* 1998; Moreau *et al.* 1999; Lee *et al.* 2002).

Another possibility to account for the more severe phenotypes conferred by the *mre11-D16A* allele is a defect in complex assembly, as shown for the *mre11-58* allele (Usui *et al.* 1998). Although the Mre11-D16A protein binds to Rad50 and Xrs2 *in vitro*, it is possible that a subtle defect in complex formation may not have been apparent at high protein concentrations (Lewis *et al.* 2004). To test these possibilities, we have compared several phenotypes, nuclease activity, and complex formation of six *mre11* mutants with substitutions of invariant residues within phosphoesterase motifs I, II, and III. All six mutants were equally impaired for the exonuclease activity of Mre11. Consistent with previous studies (Furuse *et al.* 1998; Lewis *et al.* 2004), we find that substitutions of Asp16 within motif I confer the most severe DNA repair and telomere length defects. However, these defects appear to be related to a deficiency in complex formation as interactions between Rad50 or Xrs2 and Mre11-D16A or Mre11-D16N are severely compromised, whereas the *mre11* alleles with less severe DNA repair and telomere maintenance defects exhibit stable complex formation.

MATERIALS AND METHODS

Media and growth conditions: Rich medium (YPD) and synthetic complete (SC) medium lacking the appropriate amino acid or nucleic acid base were prepared as described previously (Sherman *et al.* 1986). Sporulation medium contained 1% potassium acetate and the appropriate amino acids or nucleic acid bases at one-fifth of the concentration used in SC medium. Yeast cells were grown at 30° unless otherwise indicated.

Yeast strains and plasmids: The strains used for this study are derivatives of W303-1A or W303-1B (Thomas and Rothstein 1989), with the exception of JEL-1 and the *mre11* derivative of JEL-1. Standard genetic methods were used to generate the strains described in Table 1. Yeast transformation was by the lithium acetate method (Ito *et al.* 1983). Strains containing Rad50 or Xrs2 C-terminal epitope tags were generated by a PCR strategy using plasmid templates (Longtine *et al.* 1998). These plasmids contain 3 copies of the HA epitope, or 13 copies of the Myc epitope, followed by a translation stop codon in tandem with the *His3MX6* gene. Gene-specific recombination replaces the native stop codon with the in-frame epitope sequences, followed by the new stop codon and the *His3MX6* gene. Recombinants were selected by growth on SC-His medium and correct integration verified by genomic PCR. Expression of the epitope-tagged Rad50 or Xrs2 proteins was verified by Western blot analysis. To replace the chromosomal *MRE11* allele with the *mre11-nd* alleles, integrating plasmids containing the *mre11-nd* alleles were linearized with *Sph*I and used to transform strain W1588-4C. The resulting Ura^+ transformants were patched onto solid rich medium and then replica plated onto medium containing 5-fluoroorotic acid (5-FOA) to select for "pop-out" events. The presence of the *mre11-nd* alleles in the resulting Ura^- cells was assessed by IR sensitivity at 900 Gy; the mutations were then confirmed by genomic PCR and DNA sequence analysis. Strain LSY1706,

TABLE 1

Yeast strains

Strain	Genotype	Source or reference
W1588-4C	*MAT***a**	R. Rothstein
W1588-4A	*MAT*α	R. Rothstein
LSY779	*MAT***a** *mre11::LEU2*	Moreau *et al.* (1999)
LSY1032	*MAT***a** *mre11-D56N*	Llorente and Symington (2004)
LSY1375	*MAT***a** *mre11-D56N, H125N*	This study
LSY1397	*MAT***a** *mre11-H125N*	This study
LSY1406	*MAT***a** *mre11-D16N*	This study
LSY1407	*MAT***a** *mre11-D56A*	This study
LSY1408	*MAT***a** *mre11-H125A*	This study
LSY1559	*MAT***a** *mre11-D16A*	This study
LSY1577	*MAT*α *RAD50-3xHA-T_{ADH1}-His3MX6*	This study
LSY1578	*MAT***a** *RAD50-3xHA-T_{ADH1}-His3MX6*	This study
LSY1579	*MAT***a** *XRS2-13xMYC-T_{ADH1}-His3MX6*	This study
LSY1585	*MAT*α *RAD50-3xHA-T_{ADH1}-His3MX6 XRS2-13xMYC-T_{ADH1}-His3MX6*	This study
LSY1587	*MAT*α *RAD50-3xHA-T_{ADH1}-His3MX6 XRS2-13xMYC-T_{ADH1}-His3MX6 mre11::LEU2*	This study
LSY1643	*MAT*α *RAD50-3xHA-T_{ADH1}-His3MX6 XRS2-13xMYC-T_{ADH1}-His3MX6 mre11-D16A*	This study
LSY1645	*MAT*α *RAD50-3xHA-T_{ADH1}-His3MX6 XRS2-13xMYC-T_{ADH1}-His3MX6 mre11-D16N*	This study
LSY1646	*MAT*α *RAD50-3xHA-T_{ADH1}-His3MX6 XRS2-13xMYC-T_{ADH1}-His3MX6 mre11-D56A*	This study
LSY1648	*MAT*α *RAD50-3xHA-T_{ADH1}-His3MX6 XRS2-13xMYC-T_{ADH1}-His3MX6 mre11-H125N*	This study
LSY1650	*MAT*α *RAD50-3xHA-T_{ADH1}-His3MX6 XRS2-13xMYC-T_{ADH1}-His3MX6 mre11-H125A*	This study
LSY1651	*MAT*α *RAD50-3xHA-T_{ADH1}-His3MX6 XRS2-13xMYC-T_{ADH1}-His3MX6 mre11-D56N, H125N*	This study
LSY1655	*MAT*α *RAD50-3xHA-T_{ADH1}-His3MX6 XRS2-13xMYC-T_{ADH1}-His3MX6 mre11-D56N*	This study
JEL1	*MAT*α *leu2 trp1 ura3-52 prb1-1122 pep4-3* Δ*his3::PGAL10-GAL4*	Austin *et al.* (1995)
LSY1706	*MAT*α *leu2 trp1 ura3-52 prb1-1122 pep4-3* Δ*his3::PGAL10-GAL4 mre11::His3MX6*	This study

All strains except JEL1 and LSY1706 are derived from W303 (*leu2-3,112 trp1-1 ura3-1 can1-100 trp1-1 ade2-1 his3-11,15 can1-100 RAD5*); only mating type and differences from this genotype are shown.

containing the *mre11::His3MX6* allele, was made by PCR-mediated gene disruption of JEL-1 (Longtine *et al.* 1998). His^+ transformants were screened for IR sensitivity and the disruption confirmed by PCR.

Plasmid pSM444 containing the *mre11-D56N* allele in the integrating vector pRS406 was described previously (Llorente and Symington 2004). Plasmids pRS406-*MRE11*, pSM438, and pSM446 were generated by cloning 2.9-kb *Kpn*I/*Sac*I fragments from pRS414-*MRE11*, pRS414-*mre11-H125N*, and pRS414-*mre11-D56N, H125N*, respectively, into pRS406 (Moreau *et al.* 1999). The *mre11-D16N*, *mre11-D56A*, and *mre11-H125A* alleles were made by site-directed mutagenesis of pRS406-*MRE11* using the GeneEditor kit (Promega). Sequences of the oligonucleotides used are available on request. Plasmid pRS406-*mre11-D16A* was made by cloning a *Pml*I/*Sph*I fragment from pTZD16A (Furuse *et al.* 1998) into *Pml*I/*Sph*I-digested pRS406-*mre11-D16N*, replacing the *mre11-D16N* mutation with *mre11-D16A*. The high-copy-number plasmids containing *mre11-nd* alleles were made by cloning 2.9-kb *Kpn*I/*Sac*I fragments from the corresponding integrating vectors into pRS426 (Christianson *et al.* 1992). The plasmids used to express and purify glutathione *S*-transferase (GST) fusion proteins were derived from pSM334, containing the *MRE11* open reading frame cloned into the GST-fusion vector, pEG(KT) (Moreau *et al.* 1999). The *mre11-D16A*, *mre11-D16N*, *mre11-D56A*, and *mre11-H125A* alleles were cloned from the integrating vectors into pSM334 using standard cloning methods. The pEG(KT) vectors expressing the Mre11-D56N and Mre11-H125N proteins were described previously (Moreau *et al.* 1999). Expression of the GST-Mre11 fusion protein restores IR resistance to the *mre11*Δ strain; expression of the GST-Mre11-nd proteins results in partial complementation of the IR sensitivity of the *mre11*Δ strain.

γ-Irradiation, methyl methanesulfonate (MMS), and hydroxyurea (HU) survival assays: Cells were grown in liquid medium to mid-log phase. The cultures were serially diluted and aliquots of each dilution were plated on solid medium. The plates were irradiated in a Gammacell-220 containing ^{60}Co (Atomic Energy of Canada) for the designated dose. The dose rate of the Gammacell-220 was 0.44 Gy/sec. The plates were incubated for 3–4 days before survivors were counted. Each strain was assayed at least three times and mean values are presented. For MMS and HU survival assays, aliquots of each dilution were spotted onto YPD plates containing the indicated amount of MMS or HU; the plates were then incubated for 3 days. The MMS and HU survival assays were repeated four times.

Physical analysis of telomere length: Physical analysis of telomere length was performed using standard Southern blot techniques as described previously (Moreau *et al.* 1999). Telomere length analysis was performed three times for each of the strains; a representative gel is shown in Figure 2. For the strains containing high-copy-number plasmids, three independent transformants were analyzed for each strain; a representative gel is shown in Figure 4.

Co-immunoprecipitation: For all immunoprecipitations, 50–100 ml of cells were grown to mid-log phase in YPD, harvested, washed twice with 20 mm Tris-HCl at pH 7.4, 200 mm NaCl, and stored at –80°. Extracts were prepared and immunoprecipitated as previously described (Strahl-Bolsinger *et al.* 1997). Equivalent amounts of total soluble protein were used for the immunoprecipitations. Anti-(α)-HA monoclonal antibodies (12CA5, Roche) were used to immunoprecipitate (IP) and detect Rad50-HA. α-MYC monoclonal antibodies (Sigma) were used to IP and detect Xrs2-MYC. His_6-Mre11 was

purified from *E. coli* as described (Furuse *et al.* 1998) and used to immunize rabbits (Sigma Genosys); crude serum was used to IP and detect Mre11. The cell lysis buffer contained 140 mm or 500 mm NaCl, as described in the text. Proteins were separated by electrophoresis in 6% polyacrylamide-SDS gels, transferred to Immobilon membranes (Millipore, Medford, MA) and probed with the antibodies described above. For all of the experiments, the IP samples were concentrated four- to sixfold relative to the crude extract samples to facilitate detection of complexes.

End-joining assay: The efficiency of plasmid end joining was measured as described previously using *Bam*HI-digested pRS416 (Boulton and Jackson 1996; Moreau *et al.* 1999).

Mre11 purification and nuclease assays: Plasmids expressing GST-Mre11 or GST-Mre11-nd proteins were used to transform an *mre11*Δ derivative of the protease-defective host strain JEL1, selecting for Ura^+ transformants. The resulting strains were grown in 50 ml minimal medium to maintain selection for the plasmid and with raffinose as a carbon source. Galactose was added to the cultures to a final concentration of 2% when the cell density was 2–3 × 10^7/ml to induce expression from the *GAL1* promoter. Cells were harvested and resuspended in 0.5 ml lysis buffer [20 mm Tris-HCl, pH 8.0; 1 mm EDTA; 500 mm NaCl; 0.1% Triton-X100; 10% glycerol (v/v); 0.5 mm PMSF; 1/1000 protease inhibitor cocktail set IV (Calbiochem)]. An equal volume of zirconia silicate beads (Biospec) was added and the cells lysed by vortexing for 10 min at 4°. The lysate was centrifuged at 3000 rpm for 5 min and the supernatant transferred to a clean tube. The zirconia silicate beads were washed once with 0.5 ml of lysis buffer and centrifuged again, and the supernatants were combined. The extract was mixed with 50 μl of glutathione-sepharose beads for 1 hr at 4° to adsorb protein to the beads. The beads were precipitated by centrifugation, and the supernatant was discarded and then washed three times with 20 vol of lysis buffer. The GST fusion proteins were eluted from the beads with 2 vol of 50 mm Tris-HCl, pH 8.0; 1 mm EDTA; 20 mm glutathione, reduced; 40% glycerol (v/v) and stored at −20°. The 3′-end-labeled DNA was prepared with [α-^{32}P]dATP and Klenow DNA polymerase by using pRS415 DNA cut with *Eco*RI. Reaction conditions were as described previously (Moreau *et al.* 1999). Release of the 3′-end label was monitored by trichloroacetic acid precipitation of the substrate DNA (Fiorentini *et al.* 1997).

RESULTS

Mutations within phosphoesterase motifs of Mre11 confer variable sensitivity to IR: The conserved phosphoesterase motifs within the N-terminal domain of Mre11 are required for the exo- and endonuclease activities *in vitro* (Furuse *et al.* 1998; Usui *et al.* 1998; Moreau *et al.* 1999; Arthur *et al.* 2004). However, the variable IR sensitivity conferred by different *mre11-nd* alleles has raised the question of whether the higher IR resistance of some mutants is due to residual nuclease activity (Furuse *et al.* 1998; Usui *et al.* 1998; Moreau *et al.* 1999; Lewis *et al.* 2004). To directly compare yeast *mre11-nd* strains, an isogenic set of strains with single-amino-acid substitutions to alanine or asparagine within the N-terminal region of Mre11 was generated. The substitutions were made at conserved residues within phosphoesterase motifs I, II, or III (Figure 1A). On the basis of the crystal structure of *P. furiosus* (Pf) Mre11, a network of eight residues coordinate two Mn^{2+} ions in the active site. Asp16 is one of three residues that coordinate one of the Mn^{2+} ions (Hopfner *et al.* 2001). The histidine mutated in the *mre11-58* allele, His213, coordinates the second Mn^{2+} ion, while Asp56 is positioned to coordinate both active site metal ions. Meanwhile, His125 is thought to stabilize the accumulating negative charge on the pentacoordinated phosphate transition intermediate.

Consistent with previous studies, the *mre11-D16A* allele conferred the most severe IR sensitivity of all the point mutations, but this strain still showed greater resistance than the *mre11*Δ strain (Figure 1B) (Furuse *et al.* 1998; Lewis *et al.* 2004). The *mre11-D16A*, *mre11-D56A*, and *mre11-H125A* mutations conferred greater sensitivity to IR than substitutions at the same residues to asparagines. As described previously, the *mre11-D56N* and *mre11-H125N* strains showed similar sensitivity to IR, which was also the case for the *mre11-D56A* and *mre11-H125A* strains (Figure 1B). Because Asp56 and His125 are thought to carry out different functions in the catalytic mechanism of Mre11, we constructed an *mre11-D56N, H125N* double mutant with the expectation that any residual nuclease activity retained by the single mutants would be reduced further by the double substitution. In all of the DNA repair assays, the *mre11-D56N, H125N* strain exhibited similar sensitivity to the strains with the single *mre11-D56N* or *mre11-H125N* mutations. The hierarchy for resistance to IR, *MRE11* > *mre11-D56N* = *mre11-H125N* = *mre11-D56N, H125N* > *mre11-D16N* = *mre11-D56A* = *mre11-H125A* > *mre11-D16A* > *mre11*Δ, was also observed for resistance to MMS (Figure 1C). All of the *mre11-nd* mutants were resistant to 50 mm HU, indicating that the nuclease activity is not important for the intra-S phase checkpoint function of Mre11 (Figure 1C). However, at 100 mm HU, the *mre11-D16A* strain exhibited reduced viability. Consistent with previous studies, none of the *mre11-nd* mutants was defective in joining of cohesive ends in a plasmid transformation assay (data not shown) (Moreau *et al.* 1999; Lewis *et al.* 2004).

Telomere length is decreased in the *mre11-D16A* and *mre11-D16N* strains: Genomic DNA was isolated from all of the strains, digested with *Xho*I, and probed for telomeric sequences. As shown previously, the *mre11*Δ strain has short telomeres while the *mre11-H125N* strain has telomeres of the same length as those of the *MRE11* strain and the *mre11-D16A* strain has telomeres of intermediate length (Figure 2) (Boulton and Jackson 1998; Moreau *et al.* 1999). We found that the *mre11-D16N* strain has telomeres slightly shorter than those of wild type, but longer than those of the *mre11-D16A* strain. Like the *mre11-H125N* strain, the *mre11-D56N* and *mre11-D56N, H125N* strains have telomeres identical in length to those of the wild-type strain. However, the *mre11-D56A* and *mre11-H125A* strains have slightly shorter telomeres than wild type, but longer than those of the *mre11-D16A* and *mre11-D16N* strains. Compared to the

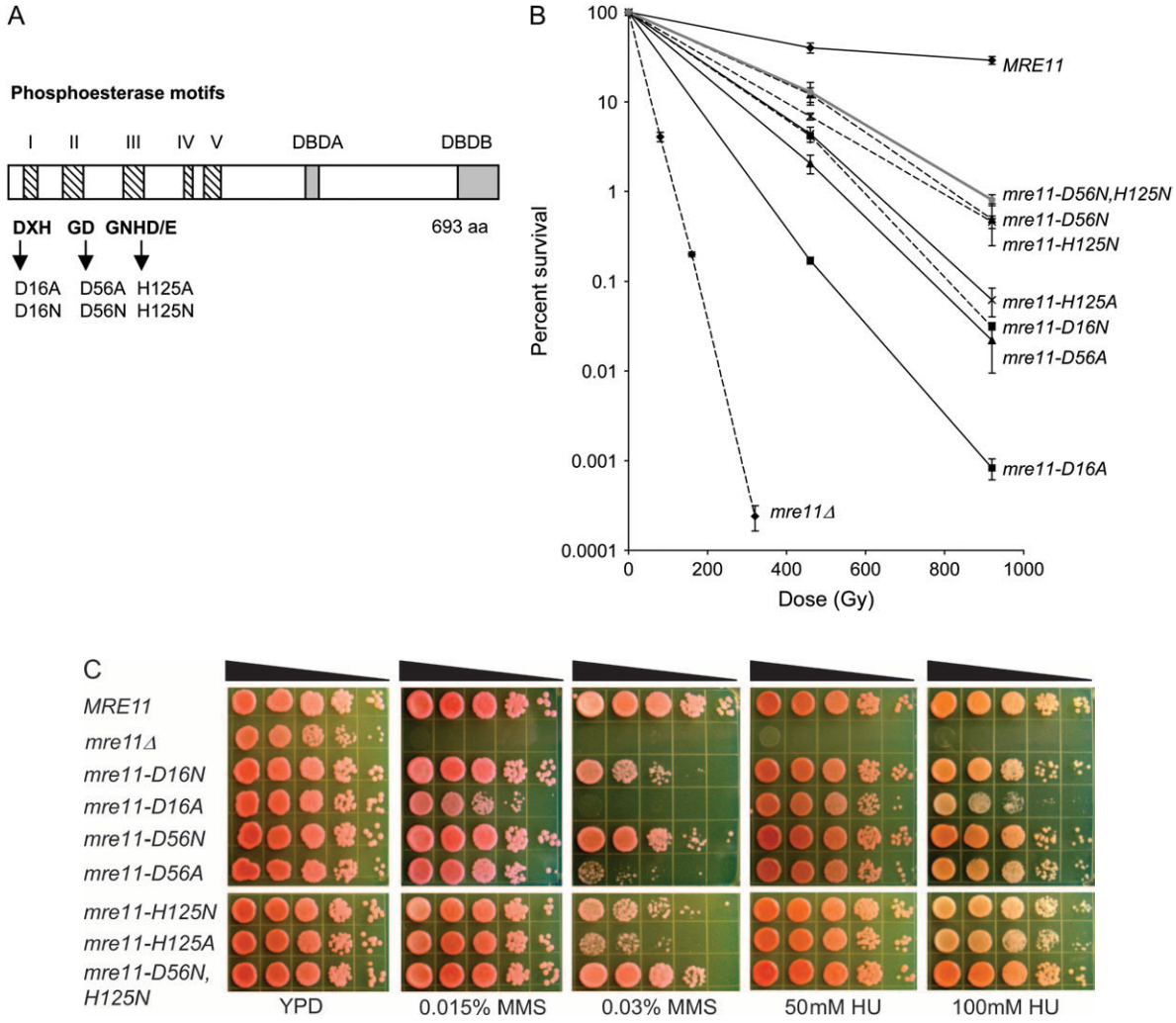

FIGURE 1.—Clastogen sensitivity of the *mre11* strains. (A) Schematic of the *Saccharomyces cerevisiae* Mre11 protein showing the conserved phosphoesterase motifs I-V and the two DNA binding domains, DBDA and DBDB (USUI *et al.* 1998). The invariant residues and substitutions at these residues in phosphoesterase motifs I, II, and III are shown. (B) Radiation sensitivity of the *mre11* strains. Dose-response curves of haploid wild-type, *mre11*Δ, and *mre11-nd* strains. (C) MMS and HU sensitivity of the *mre11* strains. Tenfold serial dilutions were spotted onto YPD plates and YPD plates containing MMS or HU at the indicated concentration.

more complex pattern of IR sensitivities, the telomere maintenance proficiencies of the motif II and III mutants suggest that residues within motif I play a more important role than residues within motifs II and III in the telomere maintenance function of Mre11.

MRX complex formation is defective in the *mre11-D16A* and *mre11-D16N* strains: We considered two possibilities for the increased IR sensitivity and short telomeres of strains with mutations in phosphoesterase motif I compared with strains with mutations in motifs II and III. First, as suggested by LEWIS *et al.* (2004), the Mre11-D16A protein might have lower residual nuclease activity than the Mre11-D56N and Mre11-H125N proteins. We consider this explanation unlikely because our previous studies indicated that the Mre11-D56N and Mre11-H125N proteins have negligible endonuclease activity and genetic studies indicate a complete defect in endonuclease activity *in vivo* in these mutants (MOREAU *et al.* 1999; RATTRAY *et al.* 2001; LOBACHEV *et al.* 2002; FARAH *et al.* 2005). Second, residues in motif I could be important for interaction of Mre11 with Rad50 and/or Xrs2, as suggested by previous two-hybrid studies (BRESSAN *et al.* 1998).

To characterize MRX complex formation by immunoprecipitation of the natively expressed proteins, the *RAD50* and *XRS2* loci were modified by the addition of C-terminal HA and MYC epitope tags, respectively (LONGTINE *et al.* 1998). These strains exhibit wild-type resistance to 500-Gy IR, but the *RAD50-HA* strain has telomeres that are slightly shorter than those of wild type (data not shown). Using α-Mre11 antibodies to immunoprecipitate Mre11, Rad50 and Xrs2 were coprecipitated with similar efficiencies in the *MRE11*, *mre11-D56A*, *mre11-D56N*, *mre11-H125A*, and *mre11-H125N* strains (Figure 3A). However, we were unable to detect MRX complex formation in the *mre11-D16A* strain, and

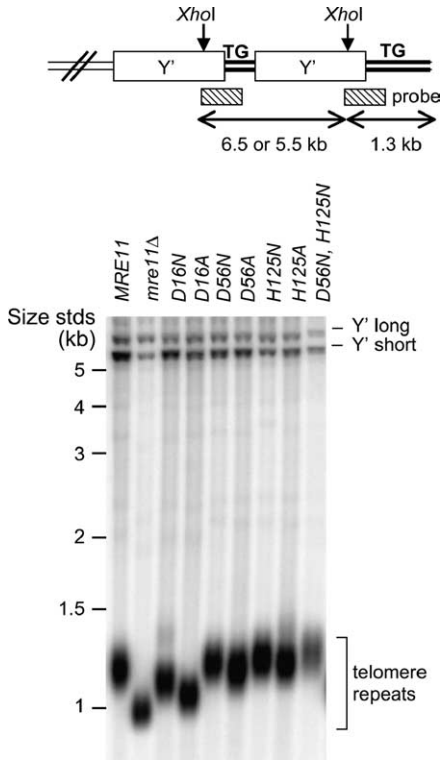

FIGURE 2.—Telomere length of the *mre11-nd* mutants. Fragments from *Xho*I-digested genomic DNA from the indicated strains were separated on a 1.2% agarose gel and the transferred fragments hybridized with a Y′ probe. The Y′ long and short subtelomeric repeat sequences are visible at the top of the gel, while the terminal fragments form heterogeneous fragments of ~1.3 kb.

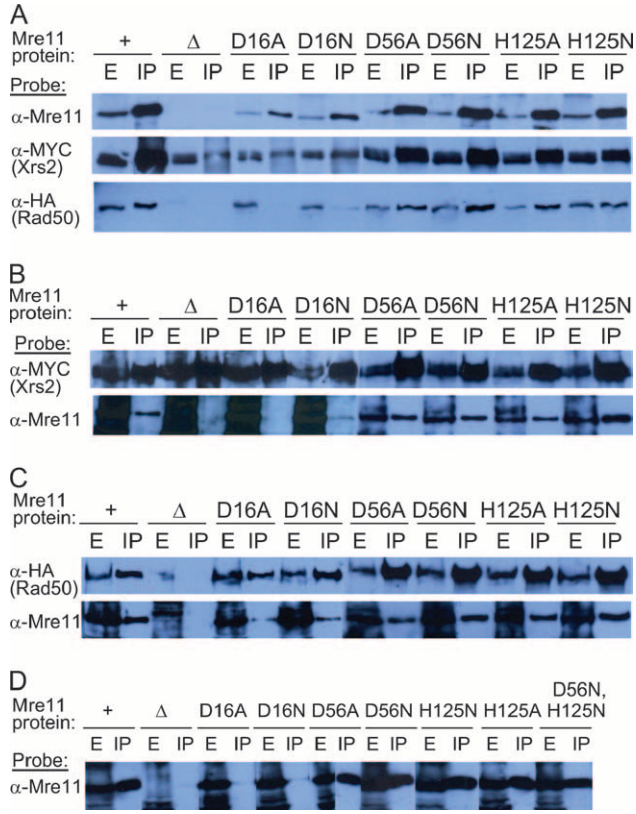

FIGURE 3.—Defect in MRX complex formation in the *mre11-D16A* and *mre11-D16N* strains. (A) Extracts prepared in 140 mM NaCl buffer were immunoprecipitated with α-Mre11 antibodies and the Western blots probed with α-Mre11, α-MYC (Xrs2), or α-HA (Rad50) antibodies as indicated. (B) Extracts prepared in 140 mM NaCl buffer were immunoprecipitated with α-MYC (Xrs2) antibodies and the Western blots probed with α-MYC or α-Mre11 antibodies. (C) Extracts prepared in 140 mM NaCl buffer were immunoprecipitated with α-HA (Rad50) antibodies and the Western blots probed with α-HA or α-Mre11 antibodies. (D) Extracts prepared in 500 mM NaCl buffer were immunoprecipitated with α-HA antibodies and the Western blots probed with α-Mre11 antibodies. The Mre11 proteins present in each strain are shown as + for wild type, Δ for the deletion strain, and by the relevant amino acid substitutions; E refers to the whole cell extract and IP refers to the immunoprecipitated proteins. IP samples were concentrated sixfold relative to the crude extract samples in A and D and fourfold relative to the crude extract samples in B and C.

there was reduced interaction between Mre11-D16N and Rad50 or Xrs2. A nonspecific band of slightly reduced mobility compared with Xrs2 was detected with the α-MYC antibodies in the *mre11*Δ and *mre11-D16N* extract immunoprecipitates. To confirm the interaction between Mre11 and Xrs2, the immunoprecipitations were repeated using α-MYC (Xrs2) antibodies (Figure 3B). Complexes were detected between Xrs2 and Mre11 in all strains except *mre11*Δ and *mre11-D16A*, and binding between Xrs2 and Mre11-D16N was reduced. Similar results were obtained for immunoprecipitations with α-HA antibodies (Rad50). A faint band corresponding to Mre11-D16A was detected in the immunoprecipitate with Rad50 indicating that binding is not completely abolished, but is greatly impaired (Figure 3C). The steady-state levels of Mre11-D16A and Mre11-D16N were similar to that of wild type, indicating that the failure to detect complexes was not due to reduced expression or stability of the mutant proteins. The immunoprecipitations were originally performed in a buffer containing 140 mM NaCl; to determine whether interaction between any of the Mre11-nd proteins and Rad50 was salt sensitive, extracts were also prepared using buffers with 500 mM NaCl. Using the high-salt buffer, there was no defect in interactions between Mre11, Mre11-D56A, Mre11-D56N, Mre11-H125A, or Mre11-H125N and Rad50 or Xrs2, but even Mre11-D16N failed to interact under these conditions (Figure 3D and data not shown). We conclude that substitutions within motif I interfere with MRX complex formation and this could account for the more severe DNA repair and telomere length defects observed for the *mre11-D16A* and *mre11-D16N* strains, compared with substitutions in motifs II and III.

Expression of *mre11-D16A* or *mre11-D16N* from high-copy-number plasmids partially suppresses the DNA repair and telomere length defects of the corresponding mutant strains: If the defect of the *mre11-D16A* and *mre11-D16N* strains is due in part to inefficient complex

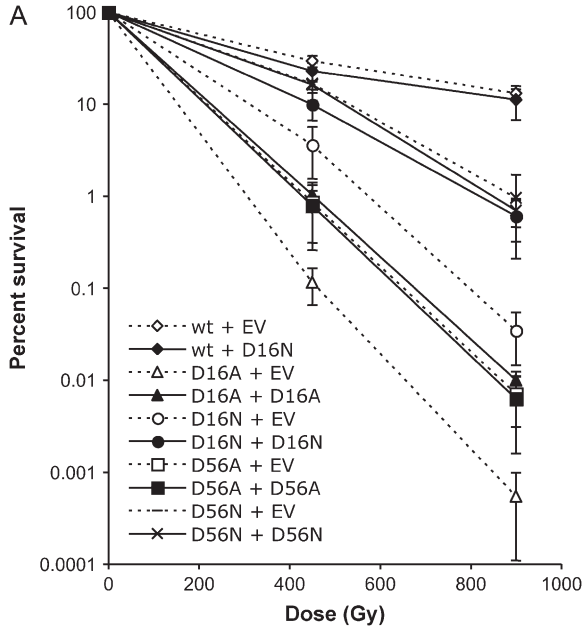

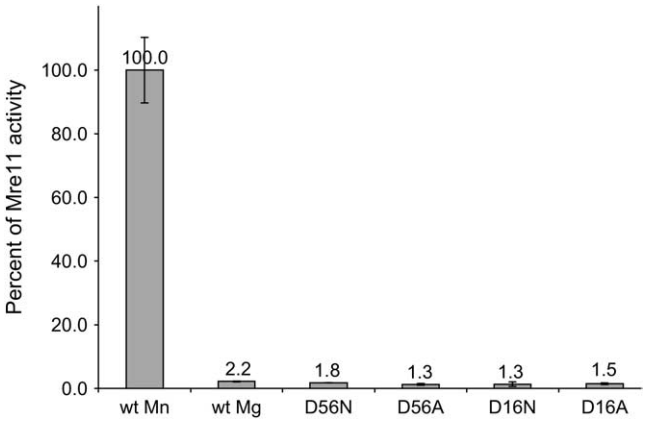

FIGURE 5.—The Asp16 and Asp56 residues are important for the Mre11 exonuclease activity. Percentage release of the 3′-end label from radiolabeled DNA fragments was determined for the partially purified proteins and normalized to the value obtained for the wild-type (wt) protein. The values for the mutant proteins in the presence of Mn^{2+} are presented.

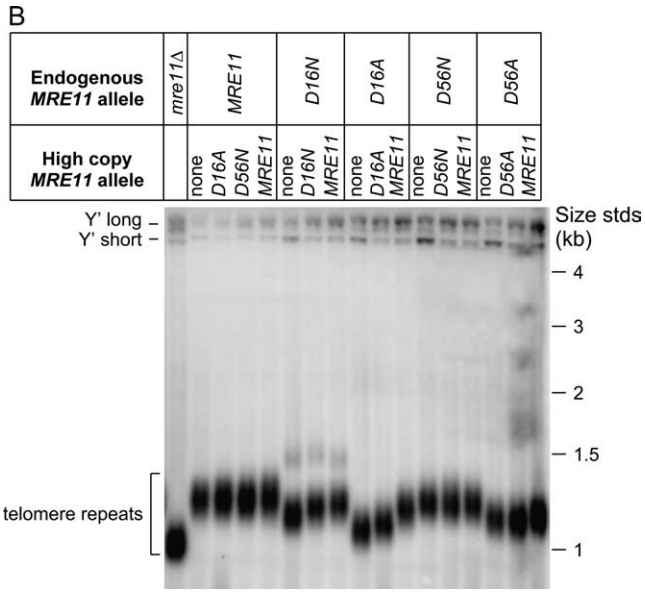

FIGURE 4.—High-copy expression of the *mre11-D16A* and *mre11-D16N* alleles partially suppresses the IR sensitivity and telomere length defect. (A) Dose-response curves for wild-type (wt), *mre11-D16A*, *mre11-D16N*, *mre11-D56A*, and *mre11-D56N* strains containing either the high-copy-number vector (EV) or high-copy-number vector with the *mre11* mutant allele. (B) Telomere length of haploid strains expressing the *mre11-nd* alleles in high copy.

formation, then one might expect partial suppression of the IR sensitivity and telomere length defect of these strains by overexpression of the mutant alleles. All of the *mre11-nd* alleles were cloned into a high-copy-number plasmid and transformed into the respective mutant strains, and the resulting transformants were tested for IR sensitivity. No suppression was observed for the *mre11-D56A*, *mre11-D56N*, *mre11-H125A*, or *mre11-H125N* alleles when present in high copy (Figure 4A, *mre11-H125N* and *mre11-H125A* not shown). In contrast, a 10- to 20-fold suppression of the IR sensitivity of the *mre11-D16A* or *mre11-D16N* strains was observed when they contained high-copy-number plasmids with the *mre11-D16A* or *mre11-D16N* alleles, respectively (Figure 4A). Furthermore, the telomere length defect of the *mre11-D16A* and *mre11-D16N* strains was partially suppressed by expression of the corresponding mutant allele from a high-copy-number vector (Figure 4B). High-copy expression of the *mre11-D56A* allele did not suppress the slight telomere length defect of the *mre11-D56A* strain. No dominant negative effects for the high-copy-number plasmids expressing the *mre11-nd* alleles in the wild-type strain were observed (only *mre11-D16N* is shown in Figure 4A).

Conserved residues within motifs I and II are required for nuclease activity: Our studies indicate that the more severe DNA repair and telomere maintenance phenotypes of the *mre11-D16N* strain compared with the *mre11-D56N* and *mre11-H125N* strains are due in part to a defect in interaction with Rad50 and Xrs2. However, we also found a significant difference between substitutions to alanine *vs.* asparagine at each of the conserved residues mutated; in each case a more severe DNA repair defect was observed for the less conservative substitutions to alanine. To determine whether the difference in phenotype is due to residual nuclease activity for the asparagine substitution mutations, the Mre11, Mre11-D16A, Mre11-D16N, Mre11-D56A, and Mre11-D56N proteins were purified from an *mre11*Δ yeast strain as fusions to GST and the 3′–5′ exonuclease activity determined by release of a 3′-end label from radiolabeled linear duplex DNA (Figure 5). The His125 mutations were not included because of the similarity in phenotype to the Asp56 mutations. As described previously (FURUSE *et al.* 1998; PAULL and GELLERT 1998; USUI *et al.* 1998; MOREAU *et al.* 1999), the Mre11 protein

exhibits Mn^{2+}-dependent 3′–5′ exonuclease activity. Approximately 2% residual nuclease activity was observed for wild-type Mre11 in the presence of Mg^{2+}; this is most likely due to the presence of contaminating nucleases because the Mre11 nuclease is Mn^{2+} dependent and the activity in the presence of Mg^{2+} was also observed for GST alone (data not shown). For all of the mutant proteins tested, the Mn^{2+}-dependent exonuclease activity was <2% of the activity observed for the wild-type protein and at the same background level seen in the presence of Mg^{2+}.

DISCUSSION

The role of the Mre11 nuclease activity in telomere maintenance and resection of DNA double-strand breaks is controversial because different nuclease-defective alleles of *MRE11* (*mre11-nd* alleles) confer variable sensitivity to IR and telomere length. The differences in phenotype could be due to residual nuclease activity for some of the mutants or to a defect in some other aspect of Mre11 function. Consistent with previous studies (Bressan *et al.* 1998; Lewis *et al.* 2004), we found a hierarchy for the *mre11-nd* strains with the *mre11-D16A* strain exhibiting the most severe phenotype, followed by the *mre11-D56A*, *mre11-H125A*, and *mre11-D16N* strains; the *mre11-D56N*, *mre11-H125N*, and *mre11-D56N, H125N* strains showed greatest DNA repair proficiency and had normal length telomeres (Figures 1 and 2). As discussed below, these differences in phenotype are due to defective complex formation for substitutions in motif I and the nature of the amino acid substitution at the conserved residues within each motif.

The Mre11-D16A and Mre11-D16N proteins are defective for complex formation *in vivo*: In a previous study, the Mre11-D16A protein was shown to bind to Rad50 and Xrs2 *in vitro* (Lewis *et al.* 2004). However, because the conditions used may have been saturating, a subtle defect in binding to the other complex components may not have been apparent. By co-immunoprecipitation of the native proteins from yeast extracts, we were unable to detect complexes between Mre11-D16A, Rad50, and Xrs2, and the Mre11-D16N protein showed less-stable complex formation (Figure 3). The conditions used for immunoprecipitation involve dilution of cellular components and therefore may accentuate interaction defects. However, complex formation for the other *mre11-nd* mutants was comparable to that of wild type, even under high salt conditions, indicating that Asp16 is essential for the integrity of the MRX complex. Consistent with reduced binding of the Mre11-D16A and Mre11-D16N proteins to Rad50 and Xrs2, the IR sensitivity and telomere length defects were partially suppressed when the mutant alleles were present in high copy (Figure 4). The IR sensitivity of the strain with the *mre11-D16A* allele in high copy was the same as the *mre11-D56A* strain; similarly, the IR sensitivity of the strain with the *mre11-D16N* allele in high copy was the same as the *mre11-D56N* strain. This observation suggests that when complex formation is restored, the DNA repair ability of strains with mutations of these conserved aspartic acid residues is the same, consistent with a similar function for Asp16 and Asp56 in coordinating active site metal ions.

The telomere length of the strain with *mre11-D16A* in high copy was not restored to the length observed in the *mre11-D56A,* suggesting that other functions at the telomere might be impaired by the *mre11-D16A* allele. A recent study showed Xrs2-dependent recruitment of Mre11 to telomeres during late S-phase, but recruitment of Mre11-D16A was reduced (Takata *et al.* 2005). Xrs2 also interacts with Tel1 and this interaction is essential for telomere maintenance, but not for DNA repair (Nakada *et al.* 2003; Tsukamoto *et al.* 2005). The only demonstrated role for Xrs2 in DNA repair is for nuclear localization of Mre11 (Tsukamoto *et al.* 2005). Therefore, it is possible that the defective interaction between Mre11-D16A and Xrs2 has a more profound effect on telomere maintenance than DNA repair. It is also possible that telomere maintenance is more sensitive to the overall level of the MRX complex than other functions. Notably, the *mre11-D16N* strain has shorter telomeres than the *mre11-D56A* strain (Figure 2), but is more resistant to IR than the *mre11-D56A* strain. Thus, the subtle defect in complex formation in the *mre11-D16N* strain may result in a telomere maintenance defect without severely compromising DNA repair. By co-immunoprecipitation, complex formation between Mre11-D16A, Rad50, and Xrs2 was greatly impaired, but the *mre11-D16A* homozygous diploid is proficient for meiotic DSB formation and NHEJ indicating that sufficient complex forms *in vivo* for these functions or that complex formation is not necessary for NHEJ and meiotic DSB formation (Furuse *et al.* 1998; Lewis *et al.* 2004). Similarly, the Mre11-58 protein is defective for Rad50 and Xrs2 interaction *in vitro*, and the *mre11-58* strain shows profound DNA repair and telomere length defects, but the *mre11-58* diploid forms meiosis-specific DSBs (Tsubouchi and Ogawa 1998). These results suggest that some functions of Mre11 have a more stringent requirement for the integrity of the MRX complex.

Role of the Mre11 nuclease activity: Lewis *et al.* (2004) suggested that the more severe DNA repair defect of the *mre11-D16A* strain, compared with the *mre11-D56N* and *mre11-H125N* strains, is due to residual nuclease activity for the Mre11-D56N and Mre11-H125N proteins. We consider this explanation unlikely. First, as discussed above, the *mre11-D16N* strain is partially defective for MRX complex formation *in vivo* and this contributes to the defects in DNA repair and telomere maintenance. Second, mutation of invariant residues in phosphoesterase motifs I or II results in a >50-fold reduction in the Mre11 exonuclease activity. We were unable to detect a difference in the residual nuclease activity between the

mutant Mre11 proteins, suggesting that the variability in phenotype of the corresponding strains is not due to higher residual nuclease activity for some of the Mre11-nd proteins (Figure 5). Extensive biochemical characterization of the Mre11-3 protein (H129L, D130V) also revealed no nuclease activity, and the phenotypes conferred by the yeast *mre11-3* and *mre11-H125N* alleles are comparable (Bressan *et al.* 1998; Lee *et al.* 2002; Arthur *et al.* 2004). The substitutions of Asp56 and His125 to asparagines were originally made because equivalent substitutions in the structurally similar λ phosphatase resulted in a 40- to 60-fold increase in the K_m of the mutant proteins for Mn^{2+} and a 10^6-fold decreased rate of hydrolysis compared with the wild-type enzyme (Zhuo *et al.* 1994). The genetic and biochemical characterization of the *mre11-nd* alleles described here is consistent with these invariant residues playing an essential role in catalysis. At all of the targeted residues, alanine substitutions resulted in a more severe defect in DNA repair and telomere maintenance compared to the more structurally and functionally conservative asparagine substitutions. The alanine substitution at position Asp16 results in a greater impairment to complex formation than the asparagine substitution, consistent with the view that the less-conservative change causes more of a structural perturbation. Although we could not detect defects in steady-state protein levels or complex formation for the Mre11-D56A and Mre11-H125A proteins, it is possible that a slight structural distortion affects some other activity of Mre11.

We were unable to detect a dominant negative phenotype by expressing the *mre11-nd* alleles in the *MRE11* strain (Figure 4 and data not shown). It is possible that the amount of the MRX complex required for DNA repair is quite low and that by increasing the copy number of the *mre11-nd* alleles by about 20-fold we were unable to compete with the endogenous protein. Mre11 is dimeric and N- and C-terminal mutations expressed in diploids show intragenic complementation indicating that heterodimers between Mre11 and Mre11-nd proteins are likely to be active (Nairz and Klein 1997; Lee *et al.* 2002).

The studies presented are consistent with the view that the *mre11-D56N* and *mre11-H125N* alleles represent true separation of function alleles because nuclease activity is greatly decreased, but MRX complex formation is intact. We have previously shown defective processing of Spo11-induced DSBs in meiosis, mild IR sensitivity, but no defect in resection of HO-induced DSBs in the *mre11-D56N* and *mre11-H125N* strains (Moreau *et al.* 2001; Llorente and Symington 2004). The *mre11-D56N* and *mre11-H125N* strains are as defective as the *mre11*Δ for the endonucleolytic processing of hairpin DNA structures *in vivo* (Rattray *et al.* 2001; Lobachev *et al.* 2002; Farah *et al.* 2005), suggesting that the primary function of the Mre11 nuclease is to cleave DNA structures or covalent adducts from DNA ends to allow subsequent processing. However, the Mre11 nuclease does not appear to play a significant role in the extensive resection of DSBs to generate long 3′-single-stranded DNA tails (Llorente and Symington 2004). Mre11 is required for formation of the short G-tails present at all telomeres in yeast, but G-tails are still present in *mre11-D56N* and *mre11-H125N* strains suggesting the Mre11 nuclease itself is not responsible for this processing step (Larrivee *et al.* 2004; Takata *et al.* 2005). The defect in formation of G-tails observed in the *mre11-D16A* strain is most likely due to reduced binding of Mre11-D16A to telomeric DNA via Xrs2 and inefficient recruitment of Rad50 (Takata *et al.* 2005).

The authors thank W. K. Holloman and L. D. Langston for critical reading of the manuscript. We thank K. Ohta, W. K. Holloman, and R. Rothstein for plasmids and strains. This work was supported by Public Health Service grant GM41784 from the National Institutes of Health and postdoctoral fellowships from the Danish Natural Science Research Council (B.O.K.), The Carlsberg Foundation (B.O.K.), and l'Association pour la Recherche sur le Cancer (B.L.).

LITERATURE CITED

Anderson, D. E., K. M. Trujillo, P. Sung and H. P. Erickson, 2001 Structure of the Rad50: Mre11 DNA repair complex from *Saccharomyces cerevisiae* by electron microscopy. J. Biol. Chem. **276:** 37027–37033.

Arthur, L. M., K. Gustausson, K. P. Hopfner, C. T. Carson, T. H. Stracker *et al.*, 2004 Structural and functional analysis of Mre11–3. Nucleic Acids Res. **32:** 1886–1893.

Austin, C. A., K. L. Marsh, R. A. Wasserman, E. Willmore, P. J. Sayer *et al.*, 1995 Expression, domain structure, and enzymatic properties of an active recombinant human DNA topoisomerase II beta. J. Biol. Chem. **270:** 15739–15746.

Boulton, S. J., and S. P. Jackson, 1996 *Saccharomyces cerevisiae* Ku70 potentiates illegitimate DNA double-strand break repair and serves as a barrier to error-prone DNA repair pathways. EMBO J. **15:** 5093–5103.

Boulton, S. J., and S. P. Jackson, 1998 Components of the Ku-dependent non-homologous end-joining pathway are involved in telomeric length maintenance and telomeric silencing. EMBO J. **17:** 1819–1828.

Bressan, D. A., H. A. Olivares, B. E. Nelms and J. H. Petrini, 1998 Alteration of N-terminal phosphoesterase signature motifs inactivates *Saccharomyces cerevisiae* Mre11. Genetics **150:** 591–600.

Carney, J. P., R. S. Maser, H. Olivares, E. M. Davis, M. Le Beau *et al.*, 1998 The hMre11/hRad50 protein complex and Nijmegen breakage syndrome: linkage of double-strand break repair to the cellular DNA damage response. Cell **93:** 477–486.

Chahwan, C., T. M. Nakamura, S. Sivakumar, P. Russell and N. Rhind, 2003 The fission yeast Rad32 (Mre11)-Rad50-Nbs1 complex is required for the S-phase DNA damage checkpoint. Mol. Cell. Biol. **23:** 6564–6573.

Chen, L., K. Trujillo, W. Ramos, P. Sung and A. E. Tomkinson, 2001 Promotion of Dnl4-catalyzed DNA end-joining by the Rad50/Mre11/Xrs2 and Hdf1/Hdf2 complexes. Mol. Cell **8:** 1105–1115.

Christianson, T. W., R. S. Sikorski, M. Dante, J. H. Shero and P. Hieter, 1992 Multifunctional yeast high-copy-number shuttle vectors. Gene **110:** 119–122.

Costanzo, V., T. Paull, M. Gottesman and J. Gautier, 2004 Mre11 assembles linear DNA fragments into DNA damage signaling complexes. PLoS Biol. **2:** E110.

D'Amours, D., and S. P. Jackson, 2001 The yeast Xrs2 complex functions in S phase checkpoint regulation. Genes Dev. **15:** 2238–2249.

D'Amours, D., and S. P. Jackson, 2002 The Mre11 complex: at the crossroads of DNA repair and checkpoint signalling. Nat. Rev. Mol. Cell. Biol. **3:** 317–327.

de Jager, M., J. van Noort, D. C. van Gent, C. Dekker, R. Kanaar *et al.*, 2001 Human Rad50/Mre11 is a flexible complex that can tether DNA ends. Mol. Cell **8:** 1129–1135.

Debrauwere, H., S. Loeillet, W. Lin, J. Lopes and A. Nicolas, 2001 Links between replication and recombination in *Saccharomyces cerevisiae*: a hypersensitive requirement for homologous recombination in the absence of Rad27 activity. Proc. Natl. Acad. Sci. USA **98:** 8263–8269.

Farah, J. A., G. Cromie, W. W. Steiner and G. R. Smith, 2005 A novel recombination pathway initiated by the Mre11/Rad50/Nbs1 complex eliminates palindromes during meiosis in *Schizosaccharomyces pombe*. Genetics **169:** 1261–1274.

Fiorentini, P., K. N. Huang, D. X. Tishkoff, R. D. Kolodner and L. S. Symington, 1997 Exonuclease I of *Saccharomyces cerevisiae* functions in mitotic recombination in vivo and in vitro. Mol. Cell. Biol. **17:** 2764–2773.

Furuse, M., Y. Nagase, H. Tsubouchi, K. Murakami-Murofushi, T. Shibata *et al.*, 1998 Distinct roles of two separable in vitro activities of yeast Mre11 in mitotic and meiotic recombination. EMBO J. **17:** 6412–6425.

Grenon, M., C. Gilbert and N. F. Lowndes, 2001 Checkpoint activation in response to double-strand breaks requires the Mre11/Rad50/Xrs2 complex. Nat. Cell. Biol. **3:** 844–847.

Haber, J. E., 1998 The many interfaces of Mre11. Cell **95:** 583–586.

Hopfner, K. P., L. Craig, G. Moncalian, R. A. Zinkel, T. Usui *et al.*, 2002 The Rad50 zinc-hook is a structure joining Mre11 complexes in DNA recombination and repair. Nature **418:** 562–566.

Hopfner, K. P., A. Karcher, L. Craig, T. T. Woo, J. P. Carney *et al.*, 2001 Structural biochemistry and interaction architecture of the DNA double-strand break repair Mre11 nuclease and Rad50-ATPase. Cell **105:** 473–485.

Ito, H., Y. Fukuda, K. Murata and A. Kimura, 1983 Transformation of intact yeast cells treated with alkali cations. J. Bacteriol. **153:** 163–168.

Larrivee, M., C. LeBel and R. J. Wellinger, 2004 The generation of proper constitutive G-tails on yeast telomeres is dependent on the MRX complex. Genes Dev. **18:** 1391–1396.

Lee, S. E., D. A. Bressan, J. H. Petrini and J. E. Haber, 2002 Complementation between N-terminal *Saccharomyces cerevisiae mre11* alleles in DNA repair and telomere length maintenance. DNA Repair (Amst.) **1:** 27–40.

Lee, S. E., J. K. Moore, A. Holmes, K. Umezu, R. D. Kolodner *et al.*, 1998 Saccharomyces Ku70, mre11/rad50 and RPA proteins regulate adaptation to G2/M arrest after DNA damage. Cell **94:** 399–409.

Lewis, L. K., F. Storici, S. Van Komen, S. Calero, P. Sung *et al.*, 2004 Role of the nuclease activity of *Saccharomyces cerevisiae* Mre11 in repair of DNA double-strand breaks in mitotic cells. Genetics **166:** 1701–1713.

Lisby, M., J. H. Barlow, R. C. Burgess and R. Rothstein, 2004 Choreography of the DNA damage response: spatiotemporal relationships among checkpoint and repair proteins. Cell **118:** 699–713.

Llorente, B., and L. S. Symington, 2004 The Mre11 nuclease is not required for 5′ to 3′ resection at multiple HO-induced double-strand breaks. Mol. Cell. Biol. **24:** 9682–9694.

Lobachev, K. S., D. A. Gordenin and M. A. Resnick, 2002 The Mre11 complex is required for repair of hairpin-capped double-strand breaks and prevention of chromosome rearrangements. Cell **108:** 183–193.

Longtine, M. S., A. McKenzie, 3rd, D. J. Demarini, N. G. Shah, A. Wach *et al.*, 1998 Additional modules for versatile and economical PCR-based gene deletion and modification in *Saccharomyces cerevisiae*. Yeast **14:** 953–961.

Moreau, S., J. R. Ferguson and L. S. Symington, 1999 The nuclease activity of Mre11 is required for meiosis but not for mating type switching, end joining, or telomere maintenance. Mol. Cell. Biol. **19:** 556–566.

Moreau, S., E. A. Morgan and L. S. Symington, 2001 Overlapping functions of the *Saccharomyces cerevisiae* Mre11, Exo1 and Rad27 nucleases in DNA metabolism. Genetics **159:** 1423–1433.

Nairz, K., and F. Klein, 1997 *mre11S*–a yeast mutation that blocks double-strand-break processing and permits nonhomologous synapsis in meiosis. Genes Dev. **11:** 2272–2290.

Nakada, D., K. Matsumoto and K. Sugimoto, 2003 ATM-related Tel1 associates with double-strand breaks through an Xrs2-dependent mechanism. Genes Dev. **17:** 1957–1962.

Nelms, B. E., R. S. Maser, J. F. MacKay, M. G. Lagally and J. H. Petrini, 1998 In situ visualization of DNA double-strand break repair in human fibroblasts. Science **280:** 590–592.

Paull, T. T., and M. Gellert, 1998 The 3′ to 5′ exonuclease activity of Mre11 facilitates repair of DNA double-strand breaks. Mol. Cell **1:** 969–979.

Rattray, A. J., C. B. McGill, B. K. Shafer and J. N. Strathern, 2001 Fidelity of mitotic double-strand-break repair in *Saccharomyces cerevisiae*: a role for *SAE2/COM1*. Genetics **158:** 109–122.

Sharples, G. J., and D. R. Leach, 1995 Structural and functional similarities between the SbcCD proteins of *Escherichia coli* and the RAD50 and MRE11 (RAD32) recombination and repair proteins of yeast. Mol. Microbiol. **17:** 1215–1217.

Sherman, F., G. R. Fink, J. B. Hicks and Cold Spring Harbor Laboratory, 1986 *Methods in Yeast Genetics*. Cold Spring Harbor Laboratory Press, Cold Spring Harbor, NY.

Strahl-Bolsinger, S., A. Hecht, K. Luo and M. Grunstein, 1997 SIR2 and SIR4 interactions differ in core and extended telomeric heterochromatin in yeast. Genes Dev. **11:** 83–93.

Symington, L. S., 2002 Role of RAD52 epistasis group genes in homologous recombination and double-strand break repair. Microbiol. Mol. Biol. Rev. **66:** 630–670.

Takata, H., Y. Tanaka and A. Matsuura, 2005 Late S phase-specific recruitment of Mre11 complex triggers hierarchical assembly of telomere replication proteins in *Saccharomyces cerevisiae*. Mol. Cell **17:** 573–583.

Thomas, B. J., and R. Rothstein, 1989 The genetic control of direct-repeat recombination in Saccharomyces: the effect of *rad52* and *rad1* on mitotic recombination at *GAL10*, a transcriptionally regulated gene. Genetics **123:** 725–738.

Tomita, K., A. Matsuura, T. Caspari, A. M. Carr, Y. Akamatsu *et al.*, 2003 Competition between the Rad50 complex and the Ku heterodimer reveals a role for Exo1 in processing double-strand breaks but not telomeres. Mol. Cell. Biol. **23:** 5186–5197.

Trujillo, K. M., and P. Sung, 2001 DNA structure-specific nuclease activities in the *Saccharomyces cerevisiae* Rad50*Mre11 complex. J. Biol. Chem. **276:** 35458–35464.

Tsubouchi, H., and H. Ogawa, 1998 A novel *mre11* mutation impairs processing of double-strand breaks of DNA during both mitosis and meiosis. Mol. Cell. Biol. **18:** 260–268.

Tsukamoto, Y., C. Mitsuoka, M. Terasawa, H. Ogawa and T. Ogawa, 2005 Xrs2p regulates Mre11p translocation to the nucleus and plays a role in telomere elongation and meiotic recombination. Mol. Biol. Cell. **16:** 597–608.

Ueno, M., T. Nakazaki, Y. Akamatsu, K. Watanabe, K. Tomita *et al.*, 2003 Molecular characterization of the *Schizosaccharomyces pombe nbs1+* gene involved in DNA repair and telomere maintenance. Mol. Cell. Biol. **23:** 6553–6563.

Usui, T., H. Ogawa and J. H. Petrini, 2001 A DNA damage response pathway controlled by Tel1 and the Mre11 complex. Mol. Cell **7:** 1255–1266.

Usui, T., T. Ohta, H. Oshiumi, J. Tomizawa, H. Ogawa *et al.*, 1998 Complex formation and functional versatility of Mre11 of budding yeast in recombination. Cell **95:** 705–716.

Uziel, T., Y. Lerenthal, L. Moyal, Y. Andegeko, L. Mittelman *et al.*, 2003 Requirement of the MRN complex for ATM activation by DNA damage. EMBO J. **22:** 5612–5621.

Varon, R., C. Vissinga, M. Platzer, K. M. Cerosaletti, K. H. Chrzanowska *et al.*, 1998 Nibrin, a novel DNA double-strand break repair protein, is mutated in Nijmegen breakage syndrome. Cell **93:** 467–476.

White, C. I., and J. E. Haber, 1990 Intermediates of recombination during mating type switching in *Saccharomyces cerevisiae*. EMBO J. **9:** 663–673.

Wiltzius, J. J., M. Hohl, J. C. Fleming and J. H. Petrini, 2005 The Rad50 hook domain is a critical determinant of Mre11 complex functions. Nat. Struct. Mol. Biol. **12:** 403–407.

Zhuo, S., J. C. Clemens, R. L. Stone and J. E. Dixon, 1994 Mutational analysis of a Ser/Thr phosphatase. Identification of residues important in phosphoesterase substrate binding and catalysis. J. Biol. Chem. **269:** 26234–26238.

Communicating editor: G. R. Smith